

# Gait analysis with multiple depth cameras

Edouard Auvinet, Franck Multon and Jean Meunier

**Abstract**—The gait movement seems simple at first glance, but in reality it is a very complex neural and biomechanical process. In particular, if a person is affected by a disease or an injury, the gait may be modified. To help detecting such change, we propose a new method based on multiple depth cameras. The aim of this paper is to show the possibility to reconstruct the body 3D volume in real time during gait in order to detect a pathological problem related to this movement and eventually improve diagnosis. Preliminary results showed that the system is sensitive to gait change produced by a heel prosthesis (heel cup) inserted in one shoe of subjects walking on a treadmill. The system detected a difference between maximal forward and backward positions of lower limbs for this pathological walk, a difference that was negligible for normal walk. These promising results were obtained with only 3 low cost depth cameras; we therefore believe that such methodology opens a new and affordable way for 3D volumetric gait analysis.

## I. INTRODUCTION

With the aging of the population, needs in healthcare will drastically increase. In this context, the development of new diagnostic tools that will be user-friendly, low cost, and easy to distribute everywhere, while remaining accurate, is imperative. This is particularly true for gait analysis. Actually, gait motion has been of interest to the scientific and medical communities for a long time [7]. To analyze gait movement, different methods already exist and are largely available. A first method uses accelerometers to record dynamics of movement. For instance they can measure gait parameters when fixed to a lumbar position [3] or to multiple locations on different limbs [5]. But those systems are intrusive and getting kinematic parameter from accelerometer is difficult due to integration errors. The gold standard to study body kinematics is the optoelectronics system that is capable to localize markers placed on body articulations with a sub-millimeter precision [12]. However those systems are very expensive and the expertise needed to use them could not permit a daily life clinical use. To lessen all these problems, markerless methods were proposed using more or less complex video camera setups and computer vision techniques [9]. Thanks to multiple cameras, a visual hull algorithm [6] can reconstruct accurately the body volume during a walk on a treadmill when at least 8 cameras are used [10]. Unfortunately this still represents a large and cumbersome experimental setup. The aim of this proposal is to present preliminary results with a new method based on

low cost depth camera such as the Kinect [1]. With a visual hull algorithm adapted for this type of sensor, we can actually reconstruct the whole 3D body on a treadmill and detect gait (possibly abnormal) change. Furthermore, this method needs only 3 depth cameras, thus offering an easy setup in any laboratory or clinic. This rest of the paper will describe the method in part II, the experimental protocol and preliminary results in part III followed by a discussion and future works in section IV.

## II. METHOD

The method can be divided into three main steps: calibration of the camera setup, 3D reconstruction from depth maps, and body volume analysis during gait.

### A. Calibration

Camera calibration is needed obtain the transformation (external parameters) between the camera coordinate system and the real world system. This is done once for all the data acquisitions. In two words, the focal length is obtain from the device [2] and this involves moving a simple plane in the measurement volume (i.e. volume enclosing the treadmill and the walker) to get the spatial relationship between cameras and the world. With the planar equation obtain for 2 cameras in at the same time, spatial relation can be computed. Once this is done, we have the following parameters: the focal length  $f_i$ , the rotation  $R_i$  and the translation  $T_i$  for each camera.

### B. Acquisition and volume reconstruction

Our system setup is composed of 3 depth cameras placed around a treadmill as shown in Fig. 3. Each camera is connected to one computer. All depth pictures are recorded with an attached timestamp given by the local computer clock. To ensure correct synchronization of the cameras, the computers are synchronized using the NTP protocol [8]. Each depth camera  $i$  returns 3D coordinates  $[x, y, Z]_i$  ( $x, y$  are image positions in the depth map and  $Z$  is the actual depth). With the calibration parameters, the 3D positions  $[X, Y, Z]_i$  in the camera  $i$  coordinate system can be computed as follows:

Then these information from all cameras are fused in the same coordinate system by transforming each point  $[x, y, Z]_i$  in the real world  $[x, y, Z]_W$  with equation 1:

$$\begin{bmatrix} X \\ Y \\ Z \end{bmatrix}_i = \begin{bmatrix} \frac{xZ}{f} \\ \frac{yZ}{f} \\ Z \end{bmatrix} \quad (1)$$

E. Auvinet is with IGB - University of Montreal, Montreal - Quebec, Canada and The M2S laboratory of Rennes 2, Rennes, France [auvinet@iro.umontreal.ca](mailto:auvinet@iro.umontreal.ca)

F. Multon, M2S laboratory of Rennes 2 [fmulton@uhb.fr](mailto:fmulton@uhb.fr)

J. Meunier, DIRO - University of Montreal, [meunier@iro.umontreal.ca](mailto:meunier@iro.umontreal.ca)

Then information from all cameras are fused in the same referential by projecting each points  $[X_i, Y_i, Z_i]_i$  in world referential  $[X, Y, Z]_W$  with equation 2

$$\begin{bmatrix} X \\ Y \\ Z \end{bmatrix}_W = R_i \begin{bmatrix} X \\ Y \\ Z \end{bmatrix}_i + T_i \quad (2)$$

Once all points from the depth image are in the real world, the 3D reconstruction can proceed. The volume reconstruction takes place in a voxelized world. This means that the measurement volume is decomposed into elementary cube with a predefined side length. In this study we chose (like [10]) a cubic voxel side length of 1 cm. The following describes the visual hull reconstruction adapted to depth camera. For each point, the vector  $\mathbf{v}$  starting from the camera optical center to the point is computed with equation 3:

$$[\mathbf{v}]_W = \begin{bmatrix} X \\ Y \\ Z \end{bmatrix}_W - T_i \quad (3)$$

Then all voxels crossed by the half line starting from the 3D point  $[X, Y, Z]_W$  with  $\mathbf{v}$  as direction vector are set to be occupied by the body volume from the camera point of view. Finally if a voxel is occupied for all (three) cameras, then this confirms that it is truly belonging to the body as shown in Fig. 1.

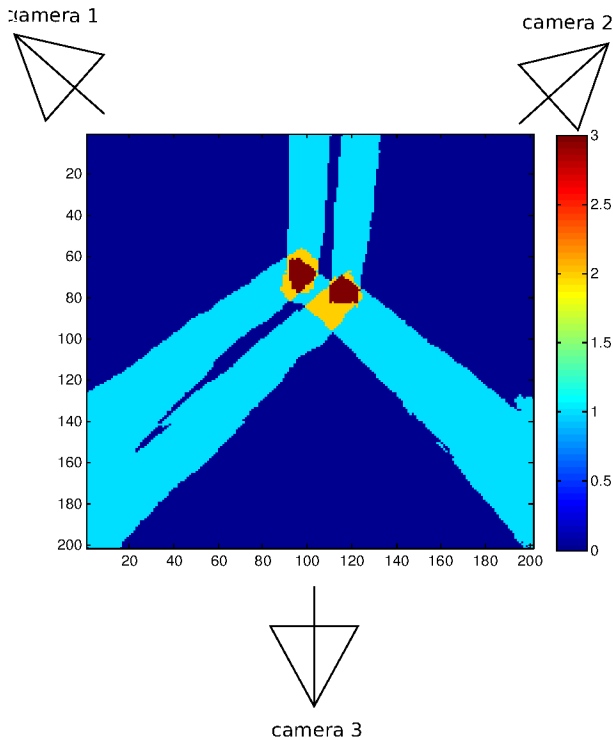


Fig. 1. Horizontal slice of the reconstructed volume with the sum of the three projected depth map.

Notice that due to the fact that in our experimental conditions, the foreground objects in the measurement space are the subject and the treadmill, the final subject's volume,

is obtained by eliminating treadmill voxels under the known treadmill height.

The centroids of each volume are then computed and all volumes are translated in order to make their centroids correspond to the center of the voxel space. This translation per frame is the movement of centroid in space and will be used later to recover gait frequency. This collection of reconstructed volumes sharing the same centroid is then ready to be analyzed.

### C. Body volume analysis

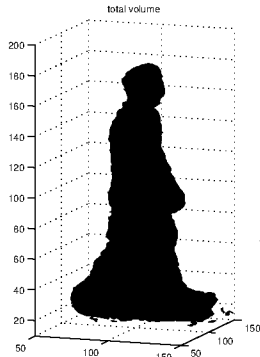
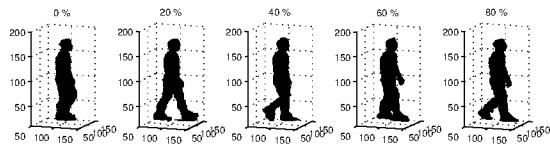
This third part consists in the analysis of the reconstructed volume. In this preliminary study we aim at measuring and comparing the left and right length of each step along the antero-posterior axis for the lower limbs. To separate each step, the gait frequency is obtained by applying a Fourier transformation on the centroid movement. Then each step is manually separated in time starting from mid stance when the two legs are together in the same frontal plane. Finally the total volume of a step is obtained by cumulating all volumes belonging to it. This total volume is analyzed slice by slice as shown in Fig. 2(a). Each slice is separated into four quadrants as shown in Fig. 2(b) that are summed laterally to obtain their projections as shown in Fig. 2(c). The forward and backward (maximal) distances of a step (w.r.t. the centroid) are measured for the left and right legs. Those (forward, backward) distances are computed and added for the (left and right) lower limbs corresponding to heights varying from -70 cm to -30 cm below the volume centroid (this corresponds to forty 1-cm slices). Analysis and comparison of these distances to study gait symmetry is tested experimentally in the next section.

## III. EXPERIMENTAL PROTOCOL AND RESULTS

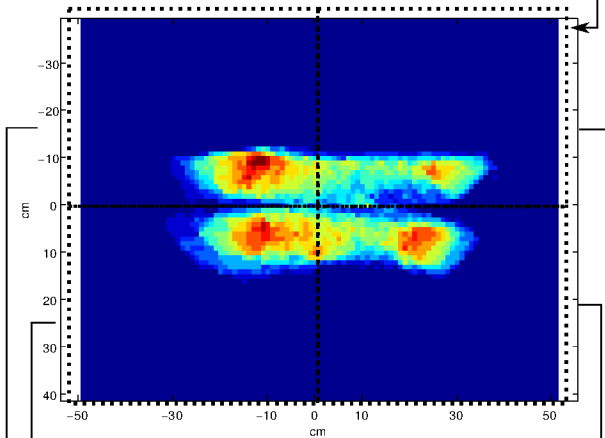
To evaluate preliminarily the validity of this symmetrical index based on volume reconstructions, we decide to compare normal gait and simulated pathological gait on 6 subjects. One on those have been dismissed because of calibration troubles. The group of 5 had the following biometric parameters : mean age of  $30.8 \pm 7.25$ , mean height  $175.6 \pm 7.77$  centimeter and a mean weight of  $76.8 \pm 13.47$  Kg. To avoid bias due to different subject's volume, each subject pass the test in normal condition following named "healthy" gait test and then with a 2.5 cm heel adapted on the left shoes and then in right shoes. Those conditions are "pathological" gait tests. The treadmill (a life fitness f3 model) was activated at the confort speed of each subject and an adaptation period of 5 minutes before the normal gait test was respected. The pathological gait tests began when the subject feels accomodate with the one side heel walk. This experiment was done with consent of local ethical commity.

The results of reconstruction process is shown in Fig. 2(a) for the entire volume and for a slice in Fig. 2(b).

As shown in Table I, with forward symmetrical index, left and right pathological gait and normal gait are separated with a standart deviation distance. Table I, Fig.4 and Fig. 5 clearly demonstrated that their is no noticable difference in



(a) Reconstructed volumes and total step volume



(b) Horizontal slice

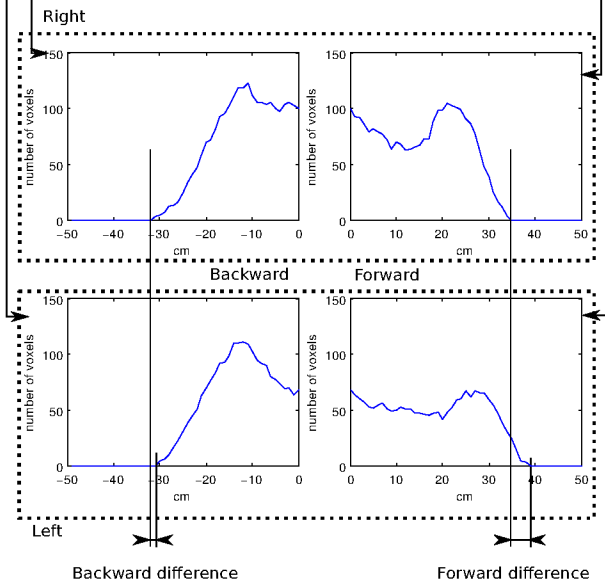


Fig. 2. Schematic representation of the volume analysis process for one slice.

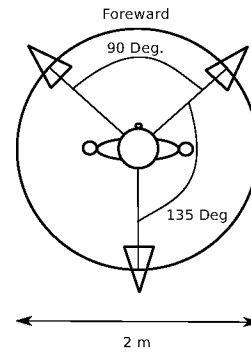


Fig. 3. Position of the 3 kinect cameras

TABLE I  
NUMERICAL RESULT OF SYMMETRY INDEX ON FORWARD AND BACKWARD

|                             | left heel | normal | right heel |
|-----------------------------|-----------|--------|------------|
| Forward mean                | 207.92    | 54.88  | -54.82     |
| Forward standard deviation  | 37.37     | 60.59  | 45.23      |
| Backward mean               | 21.86     | -15.76 | -27.26     |
| Backward standard deviation | 65.06     | 45.60  | 72.40      |

backward maximal position in contrary of forward position were the pathological gait and normal one are distinct.

#### IV. DISCUSSION AND FUTURE WORKS

The calibration procedure is a key point in order to get consistent volume reconstruction. The reconstruction process is not actually optimised and took only around a second per frame. The fact that no background model is used let this system easily usable. This new method is able to detect pathological gait introduced by a heel with measurement of step's length difference of longer (heeled leg) and shorter limb (normal leg). The step length of the heeled leg is longer than the shorter leg. This result is in the same way than leg length discrepancy problem described in [4]. We can note the fact that this difference is forward (as shown in Fig. 4) than backward (as shown in Fig. 5). This could be explain by the fact that in maximal backward position which is toe off,

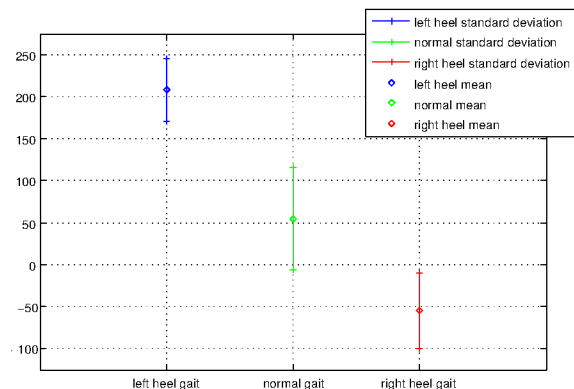


Fig. 4. Result of symmetrical index on forward

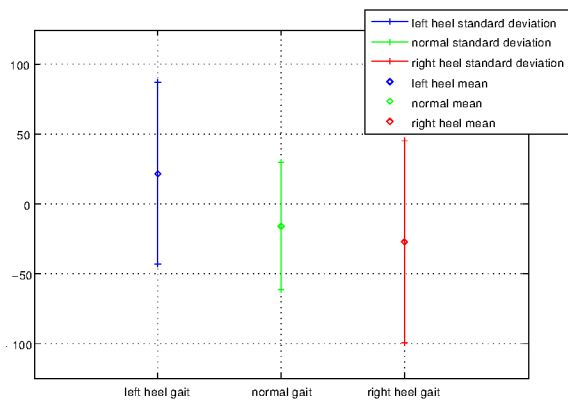


Fig. 5. Result of symmetrical index on backward

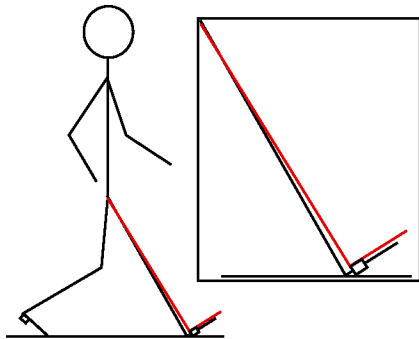


Fig. 6. Graphical representation of the heel impact on maximal position.

the heel do not interfere in the gait in contrary of forward maximal position which is heel strike (as shown in Fig. 6). The value of symmetrical index in normal gait which are low but not null is reminding that gait is always asymmetrical in small range as described in [11].

## V. CONCLUSIONS

Thanks to those results, this new method seems relevant to detect symmetrical gait troubles. Even if only three active cameras were used, reconstructed volumes was good enough to permit, associated with this symmetrical index based on difference of maximal leg position, the detection of deformation due to a 2.5 heel centimeter height. This method seems promising and interesting to be developed for considering troubles noted in the discussion.

## VI. ACKNOWLEDGMENTS

The authors gratefully acknowledge thanks for the participation of Caroline Rougier for experiments help and all subjects who participated to the experiment. This work was not supported by ANRT and FQRNT projects.

## REFERENCES

- [1] Kinect. <http://www.xbox.com/kinect>.
- [2] Openni. <http://www.openni.org>.
- [3] B. Auvinet, G. Berrut, C. Touzard, L. Moutel, N. Collet, D. Chaleil, and E. Barrey. Reference data for normal subjects obtained with an accelerometric device. *Gait & Posture*, 16(2):124–134, 2002.
- [4] B. Gurney. Leg length discrepancy. *Gait & Posture*, 15(2):195–206, 2002.

- [5] J. J. Kavanagh, S. Morrison, D. A. James, and R. Barrett. Reliability of segmental accelerations measured using a new wireless gait analysis system. *Journal of Biomechanics*, 39(15):2863–2872, 2006.
- [6] A. Laurentini. The visual hull concept for silhouette-based image understanding. *IEEE Trans. Pattern Analysis and Machine Intelligence*, pages 150–162, 1994.
- [7] É.-J. Marey. Études pratiques sur la marche de l’homme. expériences faites à la station physiologique du parc des princes. *La Nature*, (608), janvier 1885.
- [8] D. Mills, U. Delaware, J. Martin, J. Burbank, and W. Kasch. Network time protocol version 4: Protocol and algorithms specification - rfc 5905. Technical report, Internet Engineering Task Force (IETF), June 2010.
- [9] G. Moeslund and E. Granum. A survey of computer vision-based human motion capture. *Computer Vision and Image Understanding*, 81(3):231–268, 2001.
- [10] L. Mundermann, S. Corazza, and T. Andriacchi. The evolution of methods for the capture of human movement leading to markerless motion capture for biomechanical applications. *Journal of Neuro-Engineering and Rehabilitation*, 3(1):6, 2006.
- [11] H. Sadeghi, P. Allard, F. Prince, and H. Labelle. Symmetry and limb dominance in able-bodied gait: a review. *Gait & Posture*, 12(1):34–45, 2000.
- [12] M. Windolf, N. Götzten, and M. Morlock. Systematic accuracy and precision analysis of video motion capturing systems—exemplified on the vicon-460 system. *Journal of Biomechanics*, 41(12):2776–2780, 2008.